

# JOURNAL OF THE AMERICAN CHEMICAL SOCIETY

## Multiple Remeasurement of Ions in Fourier-Transform Mass Spectrometry

Evan R. Williams, Kent D. Henry, and Fred W. McLafferty\*

Contribution from the Department of Chemistry, Baker Laboratory, Cornell University, Ithaca, New York 14853-1301. Received November 27, 1989.  
Revised Manuscript Received March 6, 1990

**Abstract:** For large ions, the sensitivity of Fourier-transform mass spectrometry (FTMS) can be greatly improved by making multiple measurements of the same ions. After excitation to a large orbit for measurement, high mass ions have the advantage that their collisions with small background molecules cause negligible scattering, so that the resulting loss of kinetic energy returns the ions to the center of their original orbits where the measurement process can be repeated. With continuous ion production using  $^{252}\text{Cf}$  plasma desorption, a signal enhancement of  $\sim 100\times$  is obtained for 1000 measurements in which any remaining ions are not (versus are) removed from the cell before each measurement. With ions desorbed by a single laser pulse, a signal/noise enhancement of  $\sim 4\times$  is obtained with 25 additional measurements. Remeasurement efficiencies of 98% have been achieved for  $m/z$  2000 ions. The time required for this collisional deactivation process is  $\sim 120$  s for  $m/z$  1164 peptide ions at  $5 \times 10^{-9}$  Torr and decreases with an increase in ion mass or cell pressure, or with a decrease in excitation power. Further, this relaxation time is dependent on ion structure; collisional cross sections are  $\sim 8\times$  larger for the  $(\text{M} + \text{Na})^+$  ion of gramicidin D ( $m/z$  1904) than for Csl clusters of comparable mass, consistent with an extended linear structure for this pentadecapeptide ion. Extension of this remeasurement technique should make possible single ion detection with FTMS.

Reduction in the sample amount required is critical to solving many important research problems, especially in biology and medicine. The high sensitivity, specificity, and structural information obtained with mass spectrometry (MS)<sup>1</sup> and tandem MS (MS/MS, MS<sup>n</sup>),<sup>2</sup> combined with new ionization methods for large ions, has made this technique increasingly valuable for analyzing molecules of biological importance. Peptides as large as jack bean urease (MW  $\sim 275\,000$ ) have been ionized by matrix assisted laser desorption (LD),<sup>3</sup> and recent developments in electrospray ionization (ESI) have made possible formation of multiply protonated molecular ions for peptides as large as 133 000 daltons.<sup>4</sup>

For high mass analysis, Fourier-transform mass spectrometry (FTMS)<sup>5-9</sup> has a number of key advantages, including simulta-

(1) Facchetti, S., Ed. *Mass Spectrometry of Large Molecules*; Elsevier: Amsterdam, 1985.

(2) McLafferty, F. W., Ed. *Tandem Mass Spectrometry*; Wiley: New York, 1983. Busch, K. L.; Glish, G. L.; McLuckey, S. A. *Mass Spectrometry/Mass Spectrometry*; VCH Publishers: Deerfield, FL, 1988.

(3) Karas, M.; Hillenkamp, F. *Anal. Chem.* **1988**, *60*, 2301-2303. Hillenkamp, F.; Karas, M. 37th ASMS Conference on Mass Spectrometry and Applied Topics, Miami Beach, FL, May 1989.

(4) Fenn, J. B.; Mann, M.; Meng, C. K.; Wong, S. F.; Whitehouse, C. M. *Science* **1989**, *246*, 64-71. Loo, J. A.; Udseth, H. R.; Smith, R. D. *Anal. Biochem.* **1989**, *176*, 404-412.

(5) Comisarow, M. B.; Marshall, A. G. *Chem. Phys. Lett.* **1974**, *25*, 282-283. Marshall, A. G. *Acc. Chem. Res.* **1985**, *18*, 316-322. Laude, D. A.; Johlman, C. L.; Brown, R. S.; Weil, D. A.; Wilkins, C. L. *Mass Spectrom. Rev.* **1986**, *58*, 483-485. Chiarelli, M. P.; McCrery, D. A.; Gross, M. L. In *Ion Formation from Organic Solids*; Benninghoven, A., Ed.; Springer-Verlag, Berlin, 1986; pp 204-208. Wilkins, C. L.; Chowdhury, A. K.; Nuwaysir, L. M.; Coates, M. L. *Mass Spectrom. Rev.* **1989**, *8*, 67-92.

(6) (a) Amster, I. J.; McLafferty, F. W.; Castro, M. E.; Russell, D. H.; Cody, R. B., Jr.; Ghaderi, S. *Anal. Chem.* **1986**, *58*, 483-485. (b) Ijames, C. F.; Wilkins, C. L. *J. Am. Chem. Soc.* **1988**, *110*, 2687-2688. (c) Cody, R. B.; Amster, I. J.; McLafferty, F. W. *Proc. Natl. Acad. Sci. U.S.A.* **1985**, *82*, 6367-6370.

(7) (a) Hunt, D. F.; Shabanowitz, J.; Yates, J. R., III; Zhu, N.-Z.; Russell, D. H.; Castro, M. E. *Proc. Natl. Acad. Sci. U.S.A.* **1987**, *84*, 620-623. (b) Hunt, D. F.; Shabanowitz, J.; Yates, J. R., III; Griffin, P. R.; Zhu, N. Z. *Anal. Chim. Acta* **1989**, *225*, 1-10. (c) Amster, J. I.; Loo, J. A.; Furlong, J. J. P.; McLafferty, F. W. *Anal. Chem.* **1987**, *59*, 313-317.

neous ion detection over a wide mass range (e.g.,  $m/z$  100–16 000),<sup>6a</sup> ultrahigh resolution (60 000 for poly(propylene oxide) at  $m/z$  5922),<sup>6b</sup> and extensive capabilities for MS<sup>n</sup>.<sup>6c,7,9</sup> A wide variety of ionization techniques for large molecules have been combined with FTMS, including LD (polymers up to MW 9700),<sup>6b,c</sup> fast atom bombardment (peptides up to 12 400, but very marginal resolution at this value),<sup>7a,b</sup> secondary ion MS (subpicomole sensitivity),<sup>7c</sup> <sup>252</sup>Cf plasma desorption (PD),<sup>8</sup> and, very recently, ESI (forming carbonic anhydrase, MW ~29 000, (M + 33H)<sup>33+</sup> ions,  $m/z$  879).<sup>9</sup>

A problem with FTMS is that the detection process itself is relatively inefficient; ~10 ions are required to produce a detectable signal,<sup>10</sup> while the electron multiplier used for conventional MS detection is capable of detecting single ions. Sensitivity is even more important at high mass, as ionization efficiency decreases with increasing molecular weight. However, one unique feature of FTMS detection which has not previously been exploited is the nondestructive nature of imaging the cyclotron ion current; ions do not strike a detector surface in the analysis. Here we find that high mass ions have minimal scattering losses, so that they can be remeasured repeatedly. This leads to greatly increased sensitivity for both MS (signal/noise gain >100×) and MS/MS. For these studies large ions have been produced in pulses by LD and continuously by PD; the rate of PD ion production is highly reproducible and shows no appreciable decay over the time period of the experiments.

### Experimental Section

**Plasma Desorption.** A prototype Nicolet FTMS-2000 operated at a field strength of 2.86 T was used in a 5 × 5 × 10 cm cell (conductance limit removed).<sup>11</sup> A 50- $\mu$ Ci <sup>252</sup>Cf source (Isotope Product Laboratories), mounted outside the front trapping plate of the FTMS cell, produced ions continuously via front surface desorption.<sup>8b,c</sup> Ions were accumulated for 1–1800 s at 3 V trapping potential, and spectra (64K data points, 500-kHz bandwidth) were collected repeatedly. Quench-on spectra were collected using electrostatic removal ("quenching", +12 V and -12 V on the two trapping plates) of ions from the cell at the start of the experimental sequence and after measurement of each spectrum; quench-off spectra were measured by eliminating the quench between measurements. A rf sweep rate of 150 Hz/ $\mu$ s (35 V peak-peak, low-to-high frequency; a high-to-low frequency sweep produces comparable PD spectra) was found to produce the largest signal for the molecular ion species of gramicidin S with both quench on and off. Plots of signal versus ion collection time per scan ( $t_B$ , the delay period between successive excite/detect events) for a 30-min total analysis time, e.g., 30 s × 60 scans, 45 s × 40 scans, etc., were generated by normalizing the signal-to-noise ratio (S/N) for each of these spectra to one scan by multiplication by  $n^{0.5}$ , where  $n$  is the number of scans in each spectrum. Increased cell pressure for some of these measurements was obtained with continuous Ar introduction.

**Laser Desorption.** With the same instrument/cell configuration, back-side laser desorption was effected using 193-nm photons from a Lumonics TE-861S ArF excimer laser.<sup>11</sup> These photons were introduced into the instrument through a hollow probe and focused (to ~1 mm × 5 mm spot size, ~6 × 10<sup>6</sup> W/cm<sup>2</sup>) onto the sample on a mesh at the cell entrance. For measuring multiple quench-off spectra from a single laser pulse, ions were electrostatically quenched from the cell, sample ions were formed by a single laser pulse, and all low mass ions were ejected using appropriate rf sweeps. This was followed by a variable delay with subsequent excitation and detection. The resulting spectrum was stored and the delay/excite/detect/store sequence repeated. Typical trapping potentials were 1.5 V during ion formation and 3–8 V for measurement.

**Samples.** Samples for PD were prepared by dissolving the sample in methanol and electrospraying this solution over a Cu probe tip previously covered with electrosprayed nitrocellulose.<sup>12</sup> Glutathione was added to

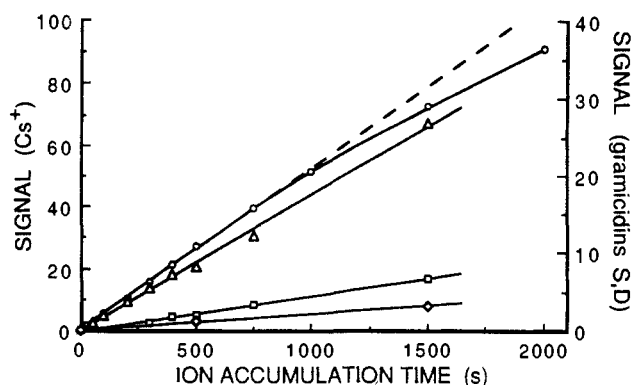


**Figure 1.** <sup>252</sup>Cf PD ion signal as a function of ion accumulation time (single measurement of accumulated ions): ○ = Cs<sup>+</sup> (dashed straight line is best fit of first 500 s); □ = (M + Na)<sup>+</sup> ( $m/z$  1164) and Δ = (ProVal + H - CO)<sup>+</sup> ( $m/z$  169) of gramicidin S; ◇ = (M + Na)<sup>+</sup> ( $m/z$  1904) of gramicidin D (18 quench-on signal-averaged measurements).

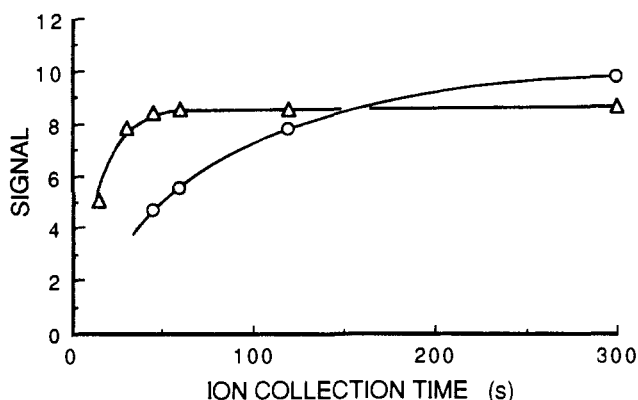


**Figure 2.** Total quench-on signal from multiple measurements over a 30-min period for  $m/z$  372 of crystal violet as a function of ion collection time between measurements; Δ = 4.5 × 10<sup>-8</sup> Torr; ○ = 1.6 × 10<sup>-8</sup> Torr.

the solutions of gramicidins S and D.<sup>13</sup> For laser desorption, samples dissolved in methanol were electrosprayed directly onto a stainless steel mesh (36% transmittance, 400 wires/in). Gramicidins S and D from Sigma were used without further purification.

### Results and Discussion

**Ion Lifetime.** For  $m/z$  169 and 1164 from gramicidin S and  $m/z$  1904 ions from gramicidin D produced by PD, the total signal increases linearly with ion accumulation time for times up to 25 min (one excite/detect event; Figure 1), consistent with even longer lifetimes for unexcited ions.<sup>8b,c</sup> On the other hand, the lower mass Cs<sup>+</sup> ions (from CsI) show significant loss of signal over this time period. As Cs<sup>+</sup> cannot dissociate and its charge exchange is unlikely (ionization potential = 3.89 eV), this loss appears to be due to ion evaporation,<sup>14</sup> enhanced with increasing ion concentration by electrostatic repulsion. Whatever the mechanism for ion loss with increasing storage time, this appears to be very low for the larger ions.

**z-Axis Collisional Deactivation.** As observed by Gross and co-workers,<sup>14</sup> ions with kinetic energy in the  $z$  axis, such as those introduced from outside the cell, can be made to produce a higher signal by collisional relaxation. Ion kinetic energy is reduced by collisions with neutral molecules which moves these ions to the  $z$ -axis center, where electrostatic inhomogeneities caused by the cell trapping plates are lower. To examine the effect of increasing the time that collisions can occur before measurement for larger ions, the total signal of  $m/z$  372 ions from crystal violet formed

(8) (a) Tabet, J. C.; Rapin, J.; Poretti, M.; Gaumann, T. *Chimia* **1986**, *40*, 169–171. (b) Loo, J. A.; Williams, E. R.; Amster, I. J.; Furlong, J. J. P.; Wang, B. H.; McLafferty, F. W. *Anal. Chem.* **1987**, *59*, 1880–1882. (c) Loo, J. A.; Williams, E. R.; Furlong, J. J. P.; Wang, B. H.; McLafferty, F. W.; Chait, B. T.; Field, F. H. *Int. J. Mass Spectrom. Ion Processes* **1987**, *78*, 305–313.

(9) Henry, K. D.; Williams, E. R.; Wang, B. H.; McLafferty, F. W.; Shabanowitz, J.; Hunt, D. F. *Proc. Natl. Acad. Sci. U.S.A.* **1989**, *86*, 9075–9078.

(10) Comisarow, M. B. *Anal. Chim. Acta* **1985**, *178*, 1–15.

(11) Williams, E. R.; Furlong, J. J. P.; McLafferty, F. W. *J. Am. Soc. Mass Spectrom.*, accepted for publication.

(12) Jonsson, G. P.; Hedin, A. B.; Hakansson, P. L.; Sundqvist, B. U. R.; Save, B. G. S.; Nielsen, P. F.; Roepstroff, P.; Johansson, K.-E.; Kamensky, I.; Lindberg, M. S. L. *Anal. Chem.* **1986**, *58*, 1084–1087.

(13) Alai, M.; Demirev, P.; Fenselau, C.; Cotter, R. J. *Anal. Chem.* **1986**, *58*, 1303–1307.

(14) Rempel, D. L.; Huang, S. K.; Gross, M. L. *Int. J. Mass Spectrom. Ion Processes* **1986**, *70*, 163–184.

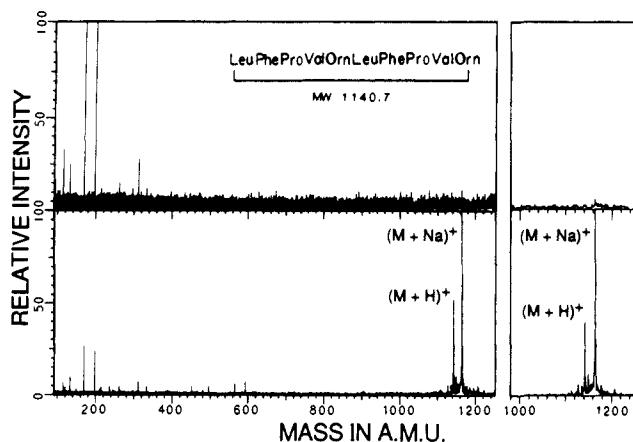


Figure 3.  $^{252}\text{Cf}$  PD spectra of gramicidin S with (left) 40 and (right, molecular ions only) 1000 scans using 45-s ion collection times (30 min total) with quench-on (top) and quench-off (bottom),  $3 \times 10^{-8}$  Torr.

by PD over a 30-min period was measured while varying the ion collection time between measurements (Figure 2). After each measurement all ions are removed from the cell (quench on), so that the total number of ions measured should be constant, independent of the ion collection time; the rate of PD ion formation is highly reproducible (Figure 1). The total signal (or S/N, with N normalized to one scan) only becomes constant with ion collection times of at least  $\sim 60$  s at a pressure of  $4.5 \times 10^{-8}$  Torr (i.e., the ions have had 0 to 60 s for collisional relaxation);  $\sim 200$  s is required at  $1.6 \times 10^{-8}$  Torr. This time is decreased by increasing the size of the ions as well as the pressure, consistent with a higher number of ion-neutral collisions, producing faster z-axis relaxation.<sup>14</sup> The total signal is also higher at the lower pressure, corresponding to the longer rf transients that this makes possible. Part of the increase in signal with increasing number of collisions could conceivably arise from relaxation of ions desorbed with excess orbital energy.

However, the time required for the total signal to become constant is inconsistent with the rate of signal increase at shorter times. For example, if ions collected for the last 45 s of a 225-s period (at  $1.6 \times 10^{-8}$  Torr) are measured with the same efficiency, 47%, as those collected for only a 45-s period (Figure 2), then the remaining 80% of the ions collected in the 225-s period would have to be measured with  $>100\%$  efficiency to obtain the observed value of 95%; if these 80% of ions stored for the first 180 s were measured with a full 100% efficiency, those collected over the last 45 s would still have to be measured with 75% efficiency to achieve the 95% overall value. This indicates that the rate of relaxation increases with higher ion concentration in the cell apparently due to ion-ion repulsion. Note that the time required for the Figure 2 signals from all ions formed during the period to reach a maximum should be approximately double that for an ion formed at the start of the period, as excited ions are being continuously introduced into the cell.

**Quench-Off Signal Enhancement.** For FTMS measurement, ions are excited into cyclotron orbits, inducing a signal in the receiver plates. This signal decays as ions are lost or become dephased, such as through collisions with background gas. It has been assumed that these ions are no longer available; the PD spectrum of gramicidin S is consistent with this for fragment ions such as  $m/z$  197 (ProVal + H) and 169 (ProVal + H - CO), which show the same total signal with or without removal of ions between the multiple scans (Figure 3). However, elimination of this quench pulse shows a dramatic effect for high mass ions, increasing  $(M + \text{Na})^+$  at  $m/z$  1164 from a S/N value of  $\sim 1$  to  $\sim 35$ . This gain in sensitivity increases with the number of scans; an improvement in S/N values from  $\sim 1.5$  to 150 can be obtained with 1000 scans (Figure 3). This effect can also be observed for ions formed by a single laser pulse, such as  $(M + \text{Na})^+$  ions from gramicidin S (Figure 4). Signal averaging five additional spectra measured 30 s apart yields a S/N gain of  $3.1 \times$  (vide infra) without further ion production.

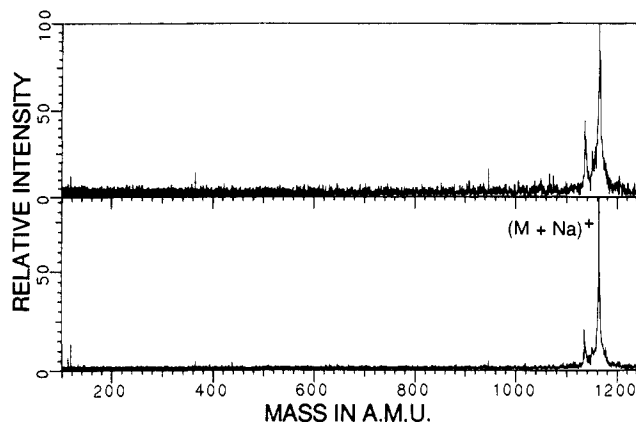


Figure 4. Laser desorption spectra of gramicidin S using a single ionization event detecting once (top), and detecting six times with 30-s delay between excite/detect events (bottom),  $3 \times 10^{-8}$  Torr.

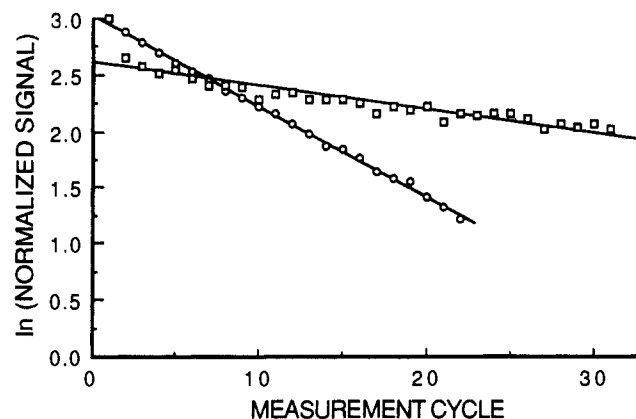
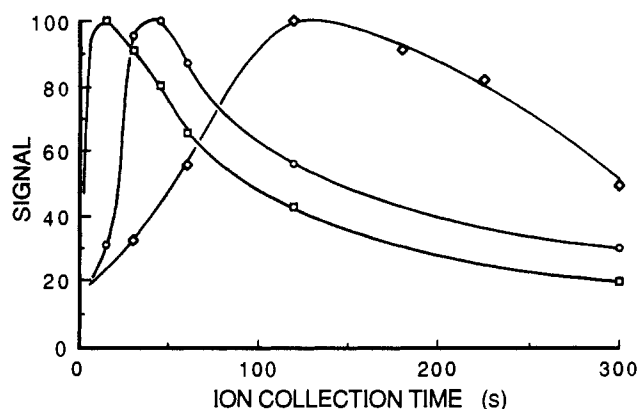


Figure 5. Signal value ( $\log_e$ ) for each remeasurement of laser-desorbed  $(M + \text{Na})^+$  ions,  $m/z$  1904, from gramicidin D, 180 s between measurements at  $9 \times 10^{-9}$  Torr. Trapping voltages:  $\circ$ , 1.5 V;  $\square$ , 8.0 V.

**xy-Plane Collisional Deactivation.** With quench off, the remeasured ions must be ones that have returned to the z axis of the cell where they are again available for excitation and detection. This suggests that collisional deactivation can take place in the xy plane, as well as along the z axis.<sup>14</sup> Each collision of an ion should reduce its kinetic energy, causing a corresponding decrease in the radius of the cyclotron orbit. Although the first collision will move the orbit center toward the point of collision, the subsequent collisions occurring at random orbit locations will have equal probabilities of moving the orbit center toward and away from the original center. Thus if a large number of collisions are required, the ion should "spiral" down to essentially the same center as that of its original orbit. Apparently, such higher mass species (Figure 3) undergo little angular scattering on collision with background molecules of 18–32 daltons, as well as little dissociation on collision because of their large number of degrees of freedom.<sup>15</sup> Despite the high proton affinities of these large ions, there is also no indication of their quench-off formation by chemical ionization or charge exchange, even when the relative concentration of low mass ions in the cell is changed dramatically.

**Ion Remeasurement Efficiency.** As a quantitative test of this effect, a single batch of  $m/z$  1904 ions from gramicidin D was generated by laser desorption and remeasured at 180-s intervals. The individual abundance values (Figure 5) show an exponential decay corresponding to 92% efficiency in each remeasurement cycle. This decay is linear over an order of magnitude change in signal. Increasing the trapping potential after ion formation and trapping from 1.5 to 8.0 V increases this efficiency to 98% (although this apparently causes ion loss after the initial mea-

(15) (a) Sheil, M. M.; Derrick, P. J. *Org. Mass Spectrom.* **1988**, *23*, 429–435. (b) Neumann, G. M.; Sheil, M. M.; Derrick, P. J. *J. Naturforsch.* **1984**, *39a*, 584–592.



**Figure 6.** Quench-off signal (same absolute scale as Figure 2) as a function of ion collection time (30 min total analysis time);  $\circ$  =  $m/z$  372 of crystal violet at  $1.6 \times 10^{-8}$  Torr;  $\square$  and  $\diamond$  =  $(M + Na)^+$  of gramicidin S ( $m/z$  1164) at  $3 \times 10^{-8}$  and  $5 \times 10^{-9}$  Torr, respectively.

surement). The increased trapping voltage could reduce the  $z$ -axis ejection induced by the chirp excitation, another possible source of ion loss.<sup>16</sup>

Thus this 2% ion loss per measurement represents that from all sources including ion dissociation; scattering losses in the remeasurement process could be much less than 2%. This is also true for another possible loss, diffusion due to the radial electric field in the cell<sup>17a</sup> (minimized with an elongated cell configuration<sup>17b</sup>). With a 98% remeasurement efficiency, a  $4.0\times$  gain in S/N is possible with 25 measurements. It is conceivable that linear ions will suffer lower scattering losses than more spherical ions of the same mass, as angular kinetic energy induced far from the charge site could be partially converted to ion vibrational energy. (For the six scans of Figure 4, the observed S/N gain of  $\sim 3.1\times$  is actually greater than that expected,  $6^{0.5} = 2.4$ , for 100% efficiency, presumably due to  $z$ -axis collisional relaxation.)

**Factors Influencing Collisional Deactivation.** When the PD  $z$ -axis-deactivation experiment (Figure 2) is rerun with quench off (Figure 6),  $m/z$  372 of crystal violet at  $1.6 \times 10^{-8}$  Torr rises far more dramatically with the increase in time available for ion collisional damping between measurements. At even longer times the total signal drops because the number of remeasurements is reduced. The same PD experiments on the larger  $m/z$  1164 of gramicidin S show this maximum moved to much shorter times, demonstrating its much faster collisional deactivation. Reducing the cell pressure from  $3 \times 10^{-8}$  to  $5 \times 10^{-9}$  Torr, on the other hand, increases the time required for this process, shifting the maximum to longer times. Decreasing the excitation power used in the measurements to 25% approximately halves the relaxation time, consistent with the lower number of collisions required to cool the ions. With short times ( $< 5$  s) between remeasurements, ions can still be remeasured although with poor efficiency; probably some portion of ions which have been collisionally depopulated can be coherently excited, despite their large cyclotron orbits.<sup>18</sup>

The overall remeasurement efficiency  $E$  for continuous PD ionization can be estimated from the Figure 6 data by compensating for the different number of measurements. The signal expected for ions collected before the first measurement scan is  $I/s$ , where  $I$  is the signal from one measurement of the ions collected over the entire 30-min period (the maximum signal in the Figure 2 quench-on plots) and  $s$  is the number of quench-off scans. The ion signal of the second scan should represent the sum of  $I/s$  for those collected during the second period plus  $E I/s$  for the remeasurement of the first period ions with an efficiency  $E$ .

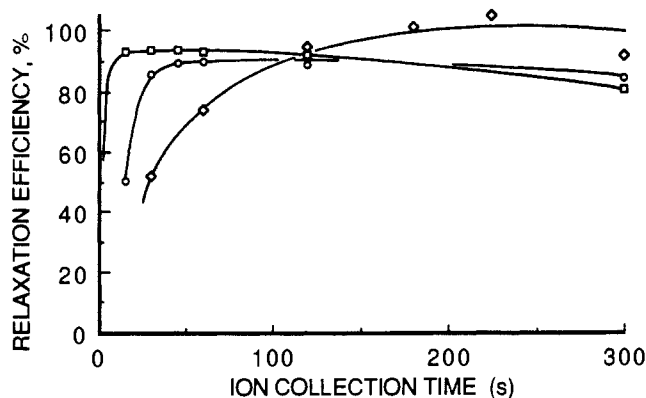


**Figure 7.** Relaxation efficiencies calculated from the data of Figure 6 using eq 1 [data for crystal violet is the average of two runs at different times, for which the value of  $(1 - \text{efficiency})$  for one run was  $\sim 60\%$  of that of the other run].

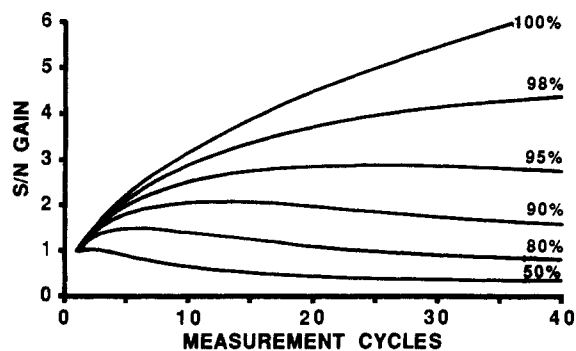


**Figure 8.** The calculated effect on the total S/N value as a function of the number of remeasurements of the ions produced by a single ionization event, showing this effect at different values (right side) of remeasurement efficiency.

Similarly, the ion signal,  $I_s$ , expected from  $s$  quench-off scans should be represented by eq 1. From this, the efficiencies for

$$\begin{aligned}
 I_s &= \{1 + [E + 1] + [(E + 1)E + 1] + \dots + \\
 &\quad [E^{s-1} + E^{s-2} + \dots + E + 1]\} I/s \\
 &= [s + (s - 1)E + (s - 2)E^2 + \dots + E^{s-1}] I/s \\
 &= I s^{-1} \sum_{i=1}^s i E^{s-i} = I [E^{s+1} - (s + 1)E + s] / s(1 - E)^2
 \end{aligned}
 \tag{1}$$

the Figure 6 data can be calculated, yielding Figure 7. Relaxation in the  $z$  axis should no longer be an important factor, as the remeasured ions should have much less  $z$ -axis excitation, and the ion concentration is much higher. Surprisingly, the relaxation time for  $m/z$  372 ion at  $1.6 \times 10^{-8}$  Torr in the  $xy$  plane is much shorter than that in  $z$  axis (Figure 2, but corrected for the continuous introduction of excited ions; vide supra), despite the much higher orbital energy induced by a chirp excitation<sup>19</sup> ( $\sim 400$  eV for  $m/z$  372). Only part can be due to the higher energy lost per collision (proportional to the ion's laboratory kinetic energy) and higher collision rate (proportional to the square root of that value). This could be an effect on the higher ion density; although the Figure 5 data show no evidence of this effect, the data could be relatively insensitive to the effect because of the extended time for collisional relaxation.

The maximum efficiencies of  $xy$  relaxation thus appear (Figure 7) to be  $>90\%$ , although the effect at longer collection times is partially obscured by increasing experimental error (we can see no other reason for the apparent decrease in efficiency with increasing time, Figure 7). An efficiency value can also be estimated from the S/N gain of  $\sim 100\times$  obtained for the  $(M + Na)^+$  of gramicidin S with 1000 scans. The decrease in ion production

(16) Huang, S. K.; Rempel, D. L.; Gross, M. L. *Int. J. Mass Spectrom. Ion Processes* **1986**, *72*, 15-31.

(17) (a) Dunbar, R. C.; Chen, J. H.; Hays, J. D. *Int. J. Mass Spectrom. Ion Processes* **1984**, *57*, 39-56. (b) Hunter, R. L.; Sherman, M. G.; McIver, R. T., Jr. *Int. J. Mass Spectrom. Ion Processes* **1983**, *50*, 259-274.

(18) Hanson, C. D.; Kerley, E. L.; Castro, M. E.; Russell, D. H. *Anal. Chem.* **1989**, *61*, 2040-2046.

(19) Cody, R. B.; Goodman, S. D.; Ghaderi, S.; Shohet, J. L. 35th ASMS Conference on Mass Spectrometry and Allied Topics, Denver, CO, May 1987.

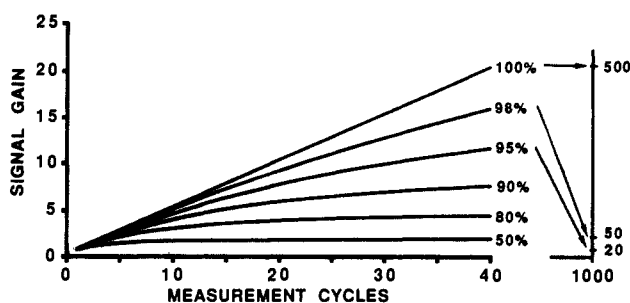


Figure 9. The calculated signal gain from using quench-off remeasurements (versus quench-on) as a function of the number of remeasurements of ions introduced continuously into the cell (as in  $^{252}\text{Cf}$  PD), showing this gain at different values (right side) of remeasurement efficiency.

rate over this long period was estimated from prior long-term measurements on the same sample, indicating a z-axis efficiency of  $\geq 50\%$  in the quench-on measurement. This leaves a signal enhancement of  $\sim 50\times$  due to  $xy$  relaxation; from eq 1 a remeasurement efficiency of 98% would result in a signal gain of  $48\times$ . Thus it would appear that the remeasurement possible with continuous ion formation is comparable to that with pulsed ion formation (Figure 5).

**Optimum Number of Remeasurements.** The remeasurement advantage is rapidly reduced with lowered efficiencies, as noise is also added with each remeasurement. For ions formed by a single pulse event showing a signal/noise value of  $S/N$  in the first measurement (Figure 8), a second measurement at 100% efficiency will increase the value to  $2S/2^{0.5}N = 1.41 S/N$ , but at 50% efficiency to only  $1.5S/2^{0.5}N = 1.06 S/N$ . A second remeasurement of the latter then gives  $1.75S/3^{0.5}N = 1.01 S/N$ , a lower value. Obviously, the optimum number of remeasurements will depend on ion mass (as well as pressure and background gas), so that an ideal data system would save partial spectra over discrete mass ranges to maximize  $S/N$  values.

This also suggests that pulsed ionization should be repeated, with sufficient sample, until the cell is filled. Ion remeasurements should then be carried out only to the point that another ionization event will just fill the cell. As an example, at 98% efficiency the  $S/N$  gain of  $4\times$  achieved in 25 remeasurements is growing very slowly (Figure 8), and 40% of the ions have been lost. If further ionization exhausting the sample only fills the cell to 75% of its original content, further remeasurements will bring the overall  $S/N$  gain to  $< 5\times$ . If only high mass information is desirable, remeasurements can be used after each ionization pulse to remove the low mass species. For continuous ionization methods, such as electrospray, that fill the ion cell in times comparable to that for  $xy$  relaxation, pulsing the sample introduction to allow sufficient remeasurement is desirable.

For continuous ionization techniques, such as plasma desorption, that require a long time to fill the cell, repeated measurements must be used to obtain significant signal levels.<sup>8</sup> Thus quench-off remeasurement does not increase the noise versus quench-on normal measurement, so that signal (and  $S/N$ ) gain from using the quench-off mode is much more dramatic (Figure 9). Again, this gain is highly dependent on efficiency. Because ions are being continuously introduced into the cell, the measurements should start immediately.

**Collisional Cross Sections.** The relaxation time should depend directly on the pressure (assuming a constant background gas composition) and the collisional cross section of the ionic species. Surprisingly, the latter can vary dramatically for singly charged ions of the same mass. With LD ionization at  $5 \times 10^{-8}$  Torr, a remeasurement efficiency of 97% (determined as in Figure 5) requires 32 s for  $(M + \text{Na})^+$  of gramicidin D ( $m/z$  1904), but requires 290 s for  $\text{Cs}_7\text{I}_6^+$  ( $m/z$  1692). Correcting for the mass difference,<sup>20a</sup> the structural differences appear to cause an 8.4-fold

change in cross section. This is consistent with the much higher masses found efficiently measurable for  $(\text{CsI})_n\text{Cs}^+$  clusters ( $m/z$  16000)<sup>6a</sup> than for peptide ions.<sup>7a</sup> A roughly cubic  $(\text{CsI})_n\text{Cs}^+$  cluster of mass 1904 would have a cross section of  $\sim 120 \text{ \AA}^2$ ,<sup>20b</sup> in the linear form this pentadecapeptide ion (assuming  $3.8 \text{ \AA}/\text{amino acid}$ )<sup>21</sup> with end groups should be  $\sim 63 \text{ \AA}$  long, so that an extended structure with an effective physical width of  $16 - 2 = 14 \text{ \AA}$  would account for this difference in cross section; a folded structure would require a larger, less realistic, width. This differs from the folded structures for keV collisions inferred by Derrick and co-workers,<sup>15b</sup> although the reported linear increase in cross section with ion mass is more consistent with a linear structure. The impressive high resolution ( $\sim 60000$ ) spectra obtained for poly(propylene glycol) ions at  $m/z$  5922<sup>6b</sup> indicate a longer rf transient in measurement of these species versus peptide ions, consistent with a less linear configuration; however, other factors,<sup>18</sup> including the number of ions in the cell, may have a significant role in transient lengths as well. We are extending these cross-section measurements.

**Application to Dissociation Techniques.** This method should also be valuable to relax ions back to the center of their orbits to make them available for dissociation. After collisionally activated dissociation (CAD) of large ions, this should make those undissociated available again for CAD; for  $(M + \text{Na})^+$  of gramicidin S formed by PD, several-fold improvements in CAD yield are observed with quench off versus quench on.<sup>22</sup> Similarly, large ions excited for measurement should be returned to the cell center with high efficiency to apply other FTMS dissociation techniques such as photodissociation,<sup>7b,11</sup> electron impact excitation of ions from organics,<sup>23</sup> and surface-induced dissociation.<sup>24</sup>

## Conclusions

The unusual nondestructive nature of FTMS detection can be exploited to enhance sensitivity by multiple remeasurements of those ions that collisionally relax back to the center of their orbits. Collisional cross sections can be inferred from the time required for this process to occur, from which physical dimensions of larger molecules in the absence of solvent can be deduced. The high efficiency of this process obtainable with large ions makes possible signal gains of  $> 100\times$  for plasma desorption. For pulsed ion introduction, such as from laser desorption or electrospray, the  $S/N$  gain is more critically dependent on remeasurement efficiency, for which values of 98% have been demonstrated here. A much more definitive picture of the relaxation process should be possible with the elegant new techniques of Marshall for measuring orbital radii and the absolute number of ions in the cell.<sup>25</sup>

For multiply charged ions, such as those with  $> 100$  charges produced by pulsed electrospray ionization,<sup>4,9</sup> any angular kinetic energy resulting from collisions with small molecules should have an even higher probability of being converted into internal vibrational energy, resulting in even lower scattering. The return of ions to the z axis might also be enhanced by a dc voltage pulse of short duration on all four excite/receive plates to create a uniform radial electric field. Improving the relaxation efficiency to 99.9% with 100 measurements would reduce the sample requirement by an order of magnitude, making possible FTMS detection of a single ion, equivalent to the sensitivity of the electron multiplier.

A unique potential of this method is the acquisition of MS and tandem MS (even  $\text{MS}^n$ ) spectra of ions produced in a single ionization event. For example, if an entire protein sample is consumed by electrospray in filling the cell with ions, initial

(20) (a) The physical dimension of these near-cubic species should vary with mass<sup>2/3</sup>, so that of a mass 1904 species should be 1.082 $\times$  that of  $\text{Cs}_7\text{I}_6^+$ . (b) An interaction distance of 1  $\text{ \AA}$  was used.

(21) Flory, P. J. *Statistical Mechanics of Chain Molecules*; Interscience: New York, 1969.

(22) Williams, E. R.; McLafferty, F. W. *J. Am. Soc. Mass Spectrom.*, accepted for publication.

(23) Cody, R. B.; Freiser, B. S. *Anal. Chem.* **1987**, *59*, 1054-1056.

(24) Ast, T.; Mabud, Md. A.; Cooks, R. G. *Int. J. Mass Spectrom. Ion Processes* **1988**, *82*, 131-150 and references cited therein. Williams, E. R.; Henry, K. D.; McLafferty, F. W.; Shabanowitz, J.; Hunt, D. F. *J. Am. Soc. Mass Spectrom.*, accepted for publication.

(25) Grosshans, P. B.; Shields, P.; Marshall, A. G. *J. Am. Chem. Soc.* **1990**, *112*, 1275-1277.

detection of the resulting ions would provide molecular weight information. After collisional relaxation, these *same* ions could be dissociated and analyzed; large daughter ions could again be relaxed, dissociated, and detected to determine their structure (using the Hadamard technique<sup>26</sup> to increase sensitivity). Even a limited sequence can allow cloning of the unknown protein, while continuing the process exploiting the MS<sup>n</sup> capabilities of FTMS

(26) Williams, E. R.; Loh, S. Y.; McLafferty, F. W.; Cody, R. B. *Anal. Chem.* 1990, 62, 698-703. For a single ionization event, the Hadamard technique could be implemented by storing ions in an elongated trap adjacent to the cell; a portion of these ions could be transferred into the cell for each Hadamard measurement.

should provide increasingly extensive sequence information concerning the original protein.

**Acknowledgment.** The authors are grateful to R. B. Cody, M. B. Comisarow, S. Ghaderi, J. A. Loo, A. G. Marshall, F. Turecek, and B. H. Wang for helpful discussions and/or experimental assistance, to Perkin-Elmer for sponsorship of an ACS Analytical Division Fellowship (for E.R.W.), and to the National Institutes of Health (Grant GM-16609) for generous financial support, and to them and the National Science Foundation (Grant CHE-8616907) for instrumentation funds.

**Registry No.** Gramicidin S, 113-73-5; gramicidin D, 1393-88-0; crystal violet, 548-62-9.

## Outer-Sphere and Inner-Sphere Processes in Reductive Elimination. Direct and Indirect Electrochemical Reduction of Vicinal Dibromoalkanes

Doris Lexa,<sup>1a</sup> Jean-Michel Savéant,<sup>\*,1a</sup> Hans J. Schäfer,<sup>\*,1b</sup> Khac-Binh Su,<sup>1a</sup> Birgit Vering,<sup>1b</sup> and Dan Li Wang<sup>1a</sup>

*Contribution from the Laboratoire d'Electrochimie Moléculaire de l'Université Paris 7, Unité Associée au CNRS N° 438, 2 place Jussieu, 75251 Paris, Cedex 05, France, and the Organisch-Chemisches Institut der Westfälischen Wilhelms Universität, Orleans Ring 23, 4400 Münster, FRG. Received October 24, 1989*

**Abstract:** The reduction of vicinal dibromoalkanes is investigated as an example of the dichotomy between outer-sphere and inner-sphere processes in reductive elimination. As a result from the analysis of the kinetic data, outer-sphere reagents such as carbon electrodes and aromatic anion radicals react with vicinal dibromoalkanes according to an "ET" mechanism in which the rate-determining step is a concerted electron-transfer bond-breaking reaction leading to the  $\beta$ -bromoalkyl radical. The latter is then reduced very rapidly, in a second step, most probably along another concerted electron-transfer bond-breaking pathway leading directly to the olefin in the heterogeneous case and through halogen atom expulsion in the homogeneous case. In the absence of steric constraints, the reduction goes entirely through the antiperiplanar conformer because the resulting  $\beta$ -bromoalkyl radical is then stabilized by delocalization of the unpaired electron over the C-C-X framework due to a favorable interaction between the  $p_x$  orbital of the radical carbon and the  $\sigma^*$  orbital of the C-Br bond. This interaction is enhanced by alkyl substitution at the reacting carbons, resulting in an approximately linear correlation between the reduction potential and the C-X bond energy of OIX<sub>2</sub> on one hand and the vertical ionization potential of the olefin on the other. The stabilization energy is of the order of 0.2-0.3 eV for the anti conformers. It can also be taken as a measure of the rotation barrier around the C-C bond responsible for the loss of stereospecificity in the reduction. This competes with the reduction of the two stable conformers of the OIX<sup>•</sup> radicals and for the expulsion of the halogen atom. There is a remarkably good agreement between the ensuing prediction of the *E:Z* olefin ratio that should be found upon reduction of threo and erythro OIX<sub>2</sub> isomers by outer-sphere reagents such as aromatic anion radicals and the experimental data. Although members of perfectly reversible redox couples, iron(I), iron("0"), and cobalt(I) porphyrins offer typical examples of inner-sphere reagents in their reaction with vicinal dibromoalkanes. They indeed react much more rapidly than outer-sphere electron donors (aromatic anion radicals) of the same standard potential. On the basis of steric hindrance experiments, it was shown that they do not react according to an S<sub>N</sub>2 rate-determining step involving the transient formation of an organometallic species. Complete stereospecificity is obtained, showing that they react along a halonium transfer E2 elimination mechanism rather than by an E1 elimination or a halogen atom transfer mechanism. As shown on a quantitative basis, this is related to the large driving force offered to halonium abstraction by the strong affinity of the iron(III) and cobalt(III) complexes toward halide ions. In regards to catalysis, the investigated systems provide typical examples showing the superiority of inner-sphere (chemical) catalysis over outer-sphere (redox) catalysis of electrochemical reactions. Not only is the catalytic efficiency much better since the rate constants of the key steps are larger, given the standard potential of the catalyst, but also selectivity is dramatically improved.

The discovery of substitution reactions involving radical anion intermediates at aliphatic<sup>2a,b</sup> and aromatic<sup>2c</sup> carbons (S<sub>RN</sub>1 reactions) as well as the development of synthetic, mechanistic, and kinetic studies in organic electrochemistry<sup>3</sup> has drawn active

attention to the role of single electron transfer—as opposed to electron pair transfer—in organic chemistry. The mechanism of the S<sub>RN</sub>1 reaction is now reasonably well understood,<sup>4</sup> even at the

(1) (a) Université de Paris 7. (b) Westfälische Wilhelms-Universität.  
(2) (a) Kornblum, N.; Michel, R. E.; Kerber, R. C. *J. Am. Chem. Soc.* 1966, 88, 5662. (b) Russell, G. A.; Danen, W. C. *J. Am. Chem. Soc.* 1966, 88, 5663. (c) Kim, J. K.; Bunnett, J. F. *J. Am. Chem. Soc.* 1970, 92, 7463.

(3) See, for example: (a) *Organic Electrochemistry*; Baizer, M. M., Lund, H., Eds.; Marcel Dekker: New York, 1983. (b) Andrieux, C. P.; Savéant, J.-M. *Electrochemical Reactions in Investigation of Rates and Mechanisms of Reactions, Techniques of Chemistry*; Bernasconi, C. F., Ed.; Wiley: New York, 1986; Vol. VI/4E, Part 2, pp 305-390.